Whole-Body Skeletal Muscle MRI Patterns in Female Dystrophinopathy Carriers

Alejandra P. Vigliano,^{1,*} Leonela Luce,^{2,3,4,*} José Manuel Pastor Rueda,⁵ Hernan Chaves,¹ Lilia Mesa,⁶ Micaela Carcione,^{2,3} Chiara Mazzanti,^{2,3} Carmen Llames Massini,^{2,3} Claudia Pamela Radic,⁷ Claudia Cejas,^{1,†} and Florencia Giliberto^{2,3,†}

Correspondence
Prof. Giliberto
gilibertoflor@gmail.com

MORE ONLINE

Supplementary Material

Neurol Genet 2025;11:e200301. doi:10.1212/NXG.0000000000200301

Abstract

Background and Objectives

Dystrophinopathies are X-linked recessive diseases caused by pathogenic variants in the *Duchenne muscular dystrophy* (*DMD*) gene. Some women carrying a single *DMD* pathogenic variant manifest variable levels of symptomatology. Those who manifest severe and early-onset symptoms are considered to be affected by dystrophinopathy rather than carriers. The aim of this study was to characterize and compare muscle structure between female *DMD* carriers who were asymptomatic at the time of the study and female control participants using whole-body MRI (WB-MRI) and correlate the findings with clinical and genetic data.

Methods

We conducted a cross-sectional observational study comparing a group of female carriers of *DMD* pathogenic variants and a group of healthy noncarrier controls. The first group included obligate and genetically confirmed *DMD* female carriers, not classified as having dystrophinopathy. Women in the healthy group had no family history of *DMD* or other muscular dystrophies. All individuals underwent WB-MRI, which was evaluated using qualitative grading scales to assess muscle edema, trophism, and fatty infiltration. Neurologic examinations, serum creatine kinase measurement, *DMD* genetic screening, and X-chromosome inactivation studies were performed on the *DMD* carriers.

Results

The study included 29 *DMD* female carriers and 30 healthy noncarrier controls. All *DMD* carriers showed signs of muscle involvement on MRI, revealing a larger proportion of skeletal muscle involvement in carriers than in controls (85% vs 27% of 48 examined muscles/group of muscles, p < 0.001). Edema, fatty infiltration, and atrophy were more common in *DMD* carriers (62.5% vs 8%; 81% vs 35%; and 81% vs 25%, respectively, all p < 0.001), particularly in muscles of the calves, thighs, and pelvic region. The most frequently affected muscles were gastrocnemius, gluteus maximus, and soleus. No correlations were found between the MRI results and the clinical and genetic data.

Discussion

Our findings indicate that *DMD* female carriers who are asymptomatic at the time of our study may be at risk of developing muscle symptoms at a future time. Multidisciplinary surveillance of *DMD* female carriers will facilitate early detection and management of complications.

This is an open access article distributed under the terms of the Creative Commons Attribution-Non Commercial-No Derivatives License 4.0 (CCBY-NC-ND), where it is permissible to download and share the work provided it is properly cited. The work cannot be changed in any way or used commercially without permission from the journal.

^{*}These authors contributed equally to this work as co-first authors.

[†]These authors contributed equally to this work as co-senior authors.

¹Departamento de Diagnóstico por Imágenes, Buenos Aires, Argentina; ²Laboratorio de Distrofinopatías, Cátedra de Genética, Facultad de Farmacia y Bioquímica, Universidad de Buenos Aires (UBA), Buenos Aires, Argentina; ³Instituto de Immunología, Genética y Metabolismo (INIGEM), CONICET-Universidad de Buenos Aires (UBA), Buenos Aires, Argentina; ⁴John Walton Muscular Dystrophy Research Centre, Translational and Clinical Research Institute, Newcastle University and Newcastle Hospitals NHS Foundation Trust, Newcastle Upon Tyne, United Kingdom; ⁵Departamento de Neurología, Buenos Aires, Argentina; ⁶Instituto de Neurociencias, Fundación Favaloro, Buenos Aires, Argentina; and ⁷Laboratorio de Genética Molecular de la Hemofilia, Instituto de Medicina Experimental (IMEX), CONICET-Academia Nacional de Medicina, Buenos Aires, Argentina.

Glossary

BMI = body mass index; **CK** = creatine kinase; **DMD** = Duchenne muscular dystrophy; **MRC** = Medical Research Council; **STIR** = short-tau inversion recovery; **WB-MRI** = whole-body MRI; **XIP** = X-chromosome inactivation pattern.

Introduction

Dystrophinopathies are X-linked recessive diseases caused by pathogenic variants in the *Duchenne muscular dystrophy* (*DMD*) gene (Xp21.2-Xp21.1; Online Mendelian Inheritance in Man ID: 300377).^{1,2} This term encompasses DMD, Becker muscular dystrophy, and *DMD*-associated dilated cardiomyopathy. Becker muscular dystrophy and DMD represent a mild-to-severe spectrum of skeletal muscle diseases.^{1,2}

According to the paradigm of X-linked recessive diseases, carrying a reference copy of the gene prevents the development of the condition, so men become affected while women are expected to be asymptomatic. However, some women carrying a single pathogenic *DMD* variant—known as "manifesting" or "female dystrophinopathy patients"—present with progressive muscle weakness and/or cardiomyopathy. A percentage of these women (2.5%–18%) exhibit muscle weakness similar to that in men, but the proportion of affected women increases from 36% to 84.3% when cardiac involvement is considered. The main genetic causes are carrying biallelic pathogenic variants in *DMD*, chromosome translocations, X-chromosome monosomy, or skewed X-chromosome inactivation affecting the "reference" allele. 4-8

The remaining women carrying a pathogenic DMD variant, referred throughout the article as DMD carriers, may show no signs/symptoms or only mild ones, such as increased serum creatine kinase (CK), myalgia, or muscle cramps. It has been demonstrated that most DMD carriers exhibit varying levels of muscle involvement, represented as increased fat fraction on MRI, and lower limb weakness compared with female noncarriers. Another MRI study evaluating 12 DMD carriers, with and without muscle weakness, revealed a consistent pattern of muscle involvement similar to that in men with DMD, albeit asymmetric.¹⁰ They observed prominent fatty infiltration in quadratus femoris, adductor magnus, biceps femoris long head, and gluteus maximus, followed by the semimembranosus, gastrocnemius medialis, and vastus, while inflammation or edema was not found. 10 However, aging and the burden of caring for patients with DMD may contribute to or exacerbate the observed signs and symptoms.

As reported in other X-linked recessive diseases, carriers can be symptomatic or asymptomatic. ¹¹⁻¹⁴ Thus, we believe that it is crucial to understand the extent and variability of signs and symptoms that female carriers may exhibit to raise awareness and improve care standards.

Taking everything into account, we hypothesized that *DMD* carriers exhibit a greater degree of skeletal muscle involvement than female noncarriers. Therefore, we aimed to characterize and compare the muscle structure of *DMD* carriers with that of healthy female controls using whole-body MRI (WB-MRI), a sensitive diagnostic technique. Furthermore, we sought to correlate the degree of skeletal muscle involvement detected by MRI with muscle strength, clinical manifestations, CK values, type of *DMD* pathogenic variants, and X-chromosome inactivation pattern (XIP).

Methods

Standard Protocol Approvals, Registrations, and Patient Consents

The study was conducted in accordance with the Declaration of Helsinki and was approved by the Institutional Review Board (or Ethics Committee) of Facultad de Farmacia y Bioquímica (06122023-167) and Fleni (1218-23). Written informed consent was obtained from all participants prior to conducting the study.

Participants

Sample size estimation for this cross-sectional observational study is described in eAppendix 1. Participants were enrolled between April 2019 and April 2022. Obligate or genetically confirmed carriers, not classified as female dystrophinopathy patients, were invited to participate in the study via the Dystrophinopathy Laboratory, FFyB/INIGEM (UBA-CONICET) (n = 183). Diagnosis of female dystrophinopathy patients was ruled out because of the absence of severe progressive muscle weakness, functional impairment, and/or cardiac involvement requiring medical intervention at the time of the invitation to the study. The first women who accepted the invitation and met the following inclusion criteria were recruited: (1) aged 18-65 years and (2) no contraindications for MRI. The control group consisted of women with no family history of dystrophinopathy or other neuromuscular disorders. They were invited to participate in this study via Fleni and the Dystrophinopathy Laboratory, FFyB/INIGEM (UBA-CONICET), and the same inclusion/ exclusion criteria were implemented.

DMD Gene Screening and Classification of Pathogenic Variants

The familial *DMD* disease-causing variants were identified prior to the study by gene screening on male proband samples. Genomic DNA was extracted from leukocytes using the cetyl-trimethyl-ammonium bromide (CTAB) method. ¹⁵ *DMD* gene

testing followed the genetic diagnostic algorithm outlined in the international best practice guidelines for dystrophinopathy genetic diagnosis, and carrier detection was performed using variant-specific tests (multiplex ligation-dependent probe amplification or PCR-Sanger sequencing). ^{16,17} No genetic studies were performed in the control group.

Variants were classified into 3 categories based on their predicted effect on dystrophin expression and function and the patient's expected phenotype: mild (partially functional dystrophin of abnormal size), moderate (nonfunctional dystrophin of abnormal size), and severe (truncating variants leading to dystrophin absence). The expected phenotype of inframe variants and the functionality of the resulting protein were based on a previous study. ¹⁸ Genotype-phenotype correlations were performed disregarding the effect of the mosaic dystrophin expression pattern in women.

Clinical Assessment

DMD carriers were clinically assessed by a neurologist specializing in neuromuscular diseases. DMD carriers were required to report (1) symptoms (e.g., myalgia, cramps, weakness, or exercise intolerance) and (2) engagement in periodic physical activity (any mild-to-moderate aerobic exercise performed for more than 30 minutes per day, 3 times a week during the past 3 months). Physical capability was assessed using the Vignos score¹⁹ while muscle strength of axial and limb muscles was manually assessed using the Medical Research Council (MRC) scale²⁰ (eTable 1). Muscle size and bulk (muscle trophism) were clinically assessed through visual inspection, palpation, and circumferential measurement to evaluate asymmetry, atrophy, and hypertrophy. Other clinical features such as craniobulbar muscle weakness, scoliosis, and retractions were also examined. Blood samples for serum CK and CK-myocardial band (CK-MB) measurements were obtained at rest, and values above 145 IU/L and 24 IU/L, respectively, were considered abnormal.

Clinical data from the control group were collected using a questionnaire administered via Google Forms (Google LLC, Menlo Park, CA), which was completed after the MRI study and reflected their self-perceived clinical status. The form can be read in eAppendix 1 while the anonymized results are given in eTable 2.

MRI Protocol

WB-MRI was acquired using a 1.5T scanner (Signa HDxt, General Electric, Milwaukee), with a body coil. MRI scans included coronal and axial T1-weighted images (T1-WI) and T2-weighted short-tau inversion recovery (STIR) images at several levels. The patients were in the supine position, with arms at their sides and palms facing upward.

Six stations were programmed with a slice thickness of 5 mm and a 5-mm gap between slices in coronal plane, at different levels including (1) head and neck; (2) shoulder girdle; (3) chest, abdomen, and upper limbs; (4) pelvic girdle; (5) thighs;

and (6) calves. Images from different stations were processed and combined in the coronal plane to reconstruct WB-MRI.

For the axial section, a 5-mm slice thickness was used, with a 10-mm gap between slices and a varying number of sections depending on each body segment. Two slices were registered at the level of the skull, 2 in the facial region, 2 at level of the neck, 3 at the shoulder girdle, 3 along the middle third of the chest, 3 at the height of the iliac crest, 3 at the level of the greater trochanter of the femur, 3 along the middle third of the thigh, and 3 along the middle third of the calf.

The following 48 muscles were evaluated:

- 1. Head: temporal, masseter, medial/lateral pterygoid, and tongue.
- 2. Neck: sternocleidomastoid, neck extensors, scapular elevator, and longus capiti.
- Shoulder girdle: latissimus dorsi, trapezius, deltoid, supraspinatus, infraspinatus, subscapularis, major and minor pectoralis, serratus anterior, and major and minor rhomboid.
- 4. Arms: anterior compartment (biceps brachii) and posterior compartment (triceps brachii).
- 5. Forearms: anterior compartment (flexor), internal compartment, and posterior compartment (extensor).
- 6. Chest/paraspinal: intercostal and dorsal paraspinal muscles.
- 7. Abdomen/paraspinals: lumbar paraspinal, piriformis, psoas iliacus, and abdominal wall.
- 8. Pelvic girdle: maximus gluteus, medius and minimus gluteus, perineal muscles, adductor magnus/large, pectineus/adductor brevis, and tensor fascia lata.
- Thighs: rectus femoris, vastus lateralis, vastus medialis, vastus intermediate, gracilis, sartorius, semimembranosus, semitendinosus, and biceps femoris short/long head.
- 10. Calves: lateral/medial gastrocnemius, soleus, anterior/posterior tibialis, extensors/flexors of the digits, and peroneal.

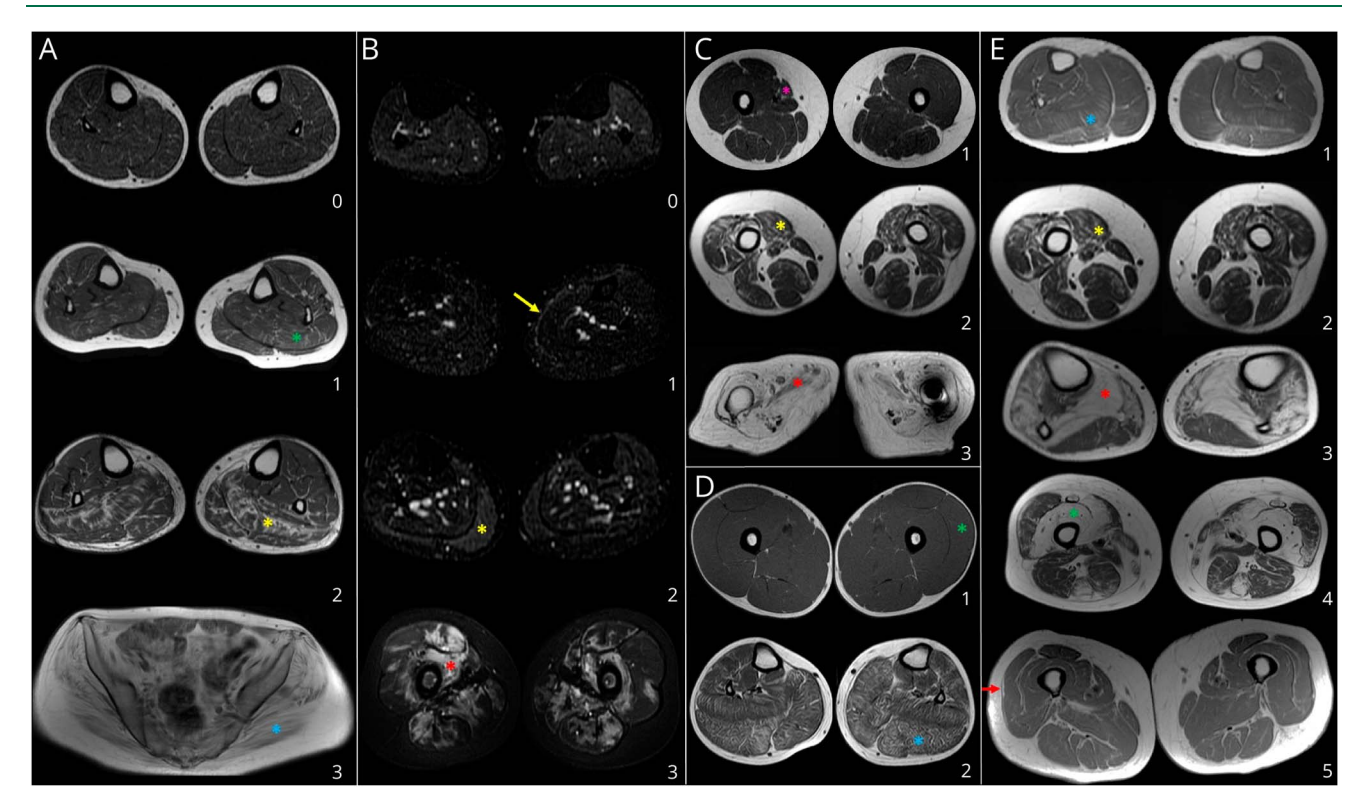
Detailed MRI planning and sequence parameters are given in eTable 3. Each study required approximately 60 minutes.

MRI Analysis

The MRI scans of all study participants were deidentified, randomized, and independently evaluated by 2 radiologists (A.P.V. and C.C.), highly experienced in neuromuscular imaging, who were blinded to the diagnosis assigned to the scans. When assessments differed, the case was re-evaluated until the 2 readers reached a consensus. The degree of involvement of each muscle group was estimated using qualitative institutional grading scales (eTable 4) applied through a standardized template (eTable 5). Five variables were evaluated for each muscle group: fatty infiltration, muscle edema, atrophy, hypertrophy/pseudohypertrophy, and muscle texture (Figure 1).

Fatty infiltration was assessed using our institutional scale, based on Mercuri's²¹ scale, on T1-WI as follows: 0 = normal

Figure 1 Qualitative Institutional Grading Scales for the 5 Variables Evaluated in WB-MRI



To illustrate the different patterns of muscle involvement, the authors provide examples from our institutional myopathy database. (A) Fatty infiltration (axial T1-WI)—0: normal muscle signal; 1: mild fatty infiltration (<30%) with bands pattern in left soleus (green asterisk); 2: moderate fatty infiltration (30%–60%) with bands pattern in left soleus (yellow asterisk); 3: severe fatty infiltration (>60%) with bands pattern in the major left gluteus muscle (blue asterisk). (B) Muscle edema (axial STIR images)—0: normal signal; 1: perifascial edema in left medial gastrocnemius (yellow arrow); 2: mild intramuscular edema in right medial gastrocnemius (yellow asterisk); and 3: severe intramuscular edema in right intermediate vastus muscle (red asterisk). (C) Atrophy (axial T1-WI)—1: mild atrophy (<30%) in right sartorius muscle (pink asterisk); 2: moderate atrophy (30%–60%) in right medial vastus muscle (yellow asterisk); 3: severe atrophy (>60%) in right long adductor muscle (red asterisk). (D) Hypertrophy/pseudohypertrophy (axial T1-WI)—1: hypertrophy in left lateral vastus muscle (green asterisk); 2: pseudohypertrophy in left lateral gastrocnemius (blue asterisk). (E) Muscle texture (axial T1-WI)—1: band pattern in right soleus (blue asterisk); 2: mottled pattern in right medial vastus muscle (yellow asterisk); 3: water band pattern in right soleus (red asterisk); 4: porcelain pattern in right intermediate vastus muscle (green asterisk); 3: water band pattern in right soleus (red asterisk); 4: porcelain pattern in right intermediate vastus muscle (green asterisk); 3: water band pattern in right soleus (red asterisk); 4: porcelain pattern in right intermediate vastus muscle (green asterisk); 3: water band pattern in right soleus (red asterisk); 4: porcelain pattern in right intermediate vastus muscle (green asterisk); 3: water band pattern in right soleus (red asterisk); 4: porcelain pattern in right intermediate vastus muscle (green asterisk); 6: porcelain pattern in right intermediate vastus muscle (red arrow)

signal and appearance, 1 = mild (small areas of high signal involving less than 30% of the muscle), 2 = moderate (areas of high signal involving between 30% and 60% of muscle), and 3 = severe (areas of high signal involving more than 60% of the muscle).

Muscle edema was graded on STIR images according to our institutional scale, as previously described 22 : 0 = normal, 1 = perifascial hypersignal (hypersignal arranged between the muscle and its fascia), 2 = mild (intramuscular hypersignal involving less than 50% of the muscle), and 3 = severe (intramuscular hypersignal involving more than 50% of the muscle).

Muscle trophism was also evaluated during neurologic examination and classified as atrophy, true hypertrophy, or pseudohypertrophy.

Atrophy was classified as follows: into 0 = normal, 1 = mild (decrease in muscle volume less than 30%), 2 = moderate (decrease in muscle volume between 30% and 60%), and 3 = severe (decrease in muscle volume more than 60%).

True hypertrophy was defined as an increase in muscle volume. Pseudohypertrophy was defined as an increase in muscle volume resulting from a rise in adipose infiltration. Trophism was classified as follows: 0 = normal, 1 = true hypertrophy, and 2 = pseudohypertrophy.

Muscle texture was only evaluated in those muscles with fatty infiltration and was classified as follows: 0 = normal, 1 = bands (linear arrangement of fatty infiltration following the longitudinal axis of the muscle), 2 = mottled (dotted arrangement of fatty infiltration), 3 = water band type (severe fatty infiltration with persistence of isolated muscle fibers), 4 = porcelain type (final stage, with severe muscle fatty infiltration where only neurovascular tissue and fascial border are distinguished), and 5 = perifascial involvement (fatty infiltration arranged between the muscle and its fascia).

Symmetric/asymmetric pattern: Symmetry was defined as all MRI variables for the muscles being affected to the same degree on both sides of the body. Alternatively, asymmetry was defined as when 1 or more MRI variables varied in the

degree of muscle involvement when comparing one side of the body with the other. The symmetric pattern was classified as 0 and the asymmetric pattern as 1.

Determination of XIP

Owing to sample availability, XIP was tested in 23 of 29 DMD carriers. Two highly polymorphic short tandem repeats in the androgen receptor (Xq12) and retinitis pigmentosa 2 (Xp11.3) genes were studied, following a previously described protocol. Allele profiles and areas under the curve were obtained from capillary electrophoresis analysis of the PCR products using GeneMarker V2.2.0 software (Softgenetics, State College, PA). XIP was determined as the median between both loci and classified as random (\leq 80%), moderately skewed (>80% and \leq 90%), and highly skewed (>90%).

Statistical Methods

Statistical analyses were performed with R version 4.2.1 in RStudio version 2023.06.1. Data from individuals with incomplete clinical assessment or MRI studies that could not be completed or presented artifacts were excluded from the analysis. Interobserver agreement of MRI results was assessed using the weighted Kappa coefficient, and owing to the high number of muscles and MRI variables evaluated, only fat infiltration of the right gluteus maximus muscles was analyzed. We considered that each MRI variable was abnormal when it was greater than 0 and that individual muscle involvement was present if at least one of the evaluated variables was abnormal. We evaluated, for the total number of DMD carriers and controls, the percentage (relative frequency) of participants in each group showing involvement of each muscle in each MRI variable. Fisher exact and χ^2 tests were used to compare the muscle structure of the DMD carriers and the control group. The Spearman rank test was used to identify correlations between the MRI and (1) the clinical assessment, (2) serum CK levels, and (3) the predicted severity of the DMD variant. For the latter 2 correlations, an index was implemented per carrier for each MRI variable, by summing the degrees of severity for the top 10 most affected muscles or all evaluated muscles, respectively. The Bonferroni method was used for adjustment of multiple comparison evaluation. Statistical significance was set at p < 0.05.

Data Availability

Investigators may request access to the anonymized individual MRI raw data by contacting Fleni. All genetic data are reported within the article and are openly available in the LOVD3 database link (databases.lovd.nl/shared/genes/DMD).

Results

Demographics and Clinical Findings

A total of 183 carriers were invited to participate in the study, and the first 30 women who accepted and met the inclusion criteria were recruited. One participant declined the MRI scan because of claustrophobia but agreed to participate in clinical

and laboratory evaluations (Figure 2) and was, therefore, excluded from the analysis.

Twenty-nine women from 20 unrelated families with a history of dystrophinopathy (13 mothers, 13 sisters, 1 aunt, and 2 grandmothers of the closest affected relative) were examined. The group's main characteristics were a mean age of 36 years (range 21-65 years) and a mean body mass index (BMI) of 28.3 kg/m^2 (range $19-45 \text{ kg/m}^2$). The control group consisted of 30 self-perceived healthy women without a family history of dystrophinopathy. However, only 25 of them completed the questionnaire regarding their clinical and demographic features. They had a mean age of 38 years (range 23-56 years) and a mean BMI of 23.1 kg/m 2 (range 17–30 kg/m 2). Differences in weight and BMI were observed between the groups (p <0.001). Approximately 50% of carriers (51.7%, n = 15) and controls (53.8%, n = 14) performed regular physical activity. DMD carriers reported symptoms more frequently than controls (55%, n = 16, vs 34%, n = 9), including weakness (17.2%, n = 5, vs 7.7%, n = 2), cramps (41.4%, n = 12, vs 19.2%, n = 5), and myalgia (24.1%, n = 7, vs 19.2%, n = 5). However, all differences were nonsignificant (p > 0.05).

Symmetric or asymmetric calf hypertrophy was clinically observed in 58.6% of DMD carriers. In addition, mild proximal muscle weakness (MRC score = 4), primarily affecting the pelvic girdle (48.3%) and shoulder girdle (17.2%), was detected. Mild cervical muscle weakness was observed in 17.2% (n = 5) of DMD carriers. Main demographic and clinical findings are summarized in Table 1 and eTable 6.

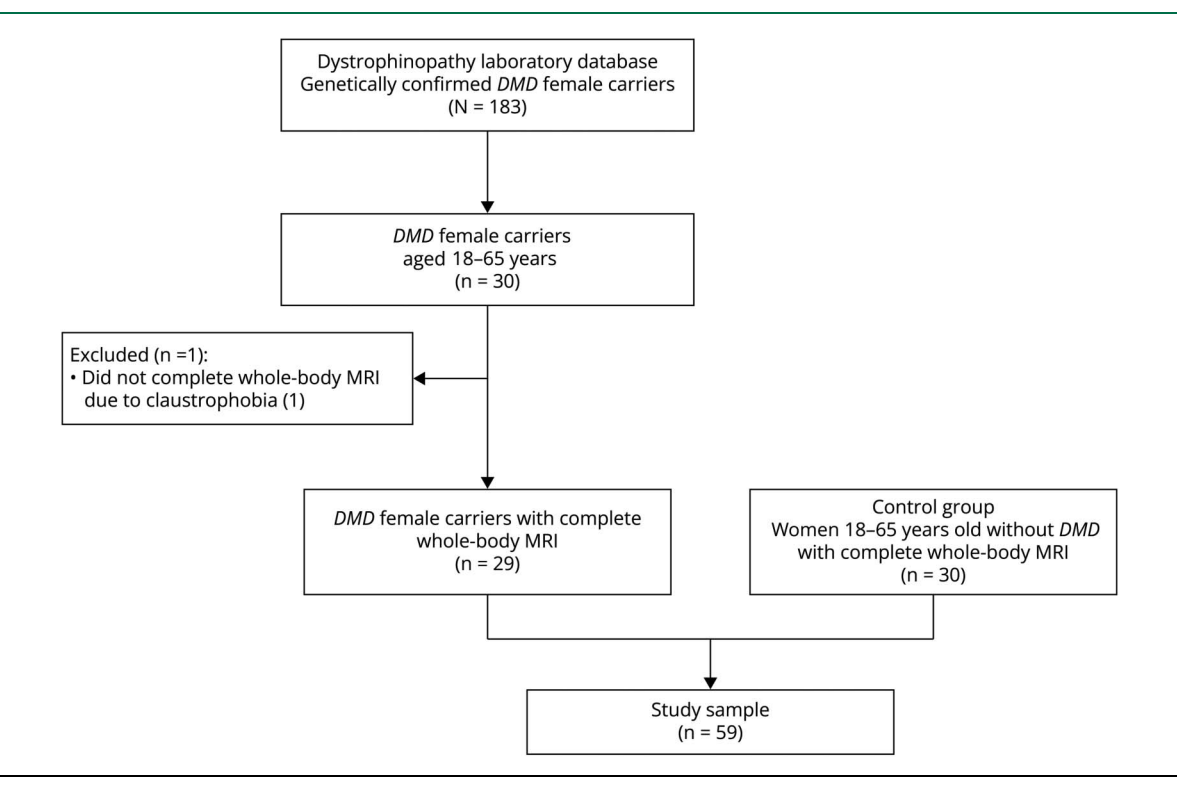
MRI Data

MRI scans of all study participants were anonymized and were blindly randomized and independently evaluated by 2 radiologists. Qualitative institutional grading scales were used to evaluate muscle edema on STIR images and fatty infiltration, atrophy, hypertrophy/pseudohypertrophy, and muscle texture on T1-WI.

The interobserver agreement between raters prior to reconciling differences in assessing the degree of muscle involvement was substantial, with a weighted Kappa coefficient value of 0.74. Female carriers demonstrated pathologic MRI variables (scores greater than zero) across a higher proportion of muscles compared with controls. Specifically, 62.5% of carrier muscles exhibited a median edema score greater than zero, compared with only 8.3% in controls (p < 0.001). Fatty infiltration was observed in 81% of muscles in carriers vs 35% in controls (p < 0.001), and atrophy was present in 81% of muscles in carriers compared with 25% in controls (p < 0.001) (Figure 3).

Initially, we compared the number of significantly altered MRI variables in each muscle group between carriers and controls. This broad analysis revealed that, in female carriers, all 5 variables were significantly affected in lateral/medial gastrocnemius, gluteus maximus, and soleus. Four variables (edema, atrophy, fatty infiltration, and texture) were significantly affected in deltoids,

Figure 2 Flowchart Showing the Inclusion and Exclusion Criteria of Study Participants at Various Stages of the Conducted Examination



gluteus medius/minimus, pectorals, peroneus, and vastus lateralis. In the latissimus dorsi and neck extensor muscles of carriers, 3 variables (atrophy, fatty infiltration, and texture pattern) were significantly altered (Figure 4).

Moreover, the percentages of edema, fatty infiltration, atrophy, and hypertrophy/pseudohypertrophy in the muscles with more variables involved, mentioned in Figure 4, were compared between groups, finding statistically significant differences in almost all the comparisons. Pseudohypertrophy was observed only in the gastrocnemius, gluteus maximus, and soleus of carriers (Table 2).

Second, for each of the 5 MRI variables, we compared the levels of involvement in each muscle group (n = 48) between DMD carriers and controls (Figure 5). From the 240 comparisons, 33% showed a statistically significant increase in muscle involvement in DMD carriers compared with controls.

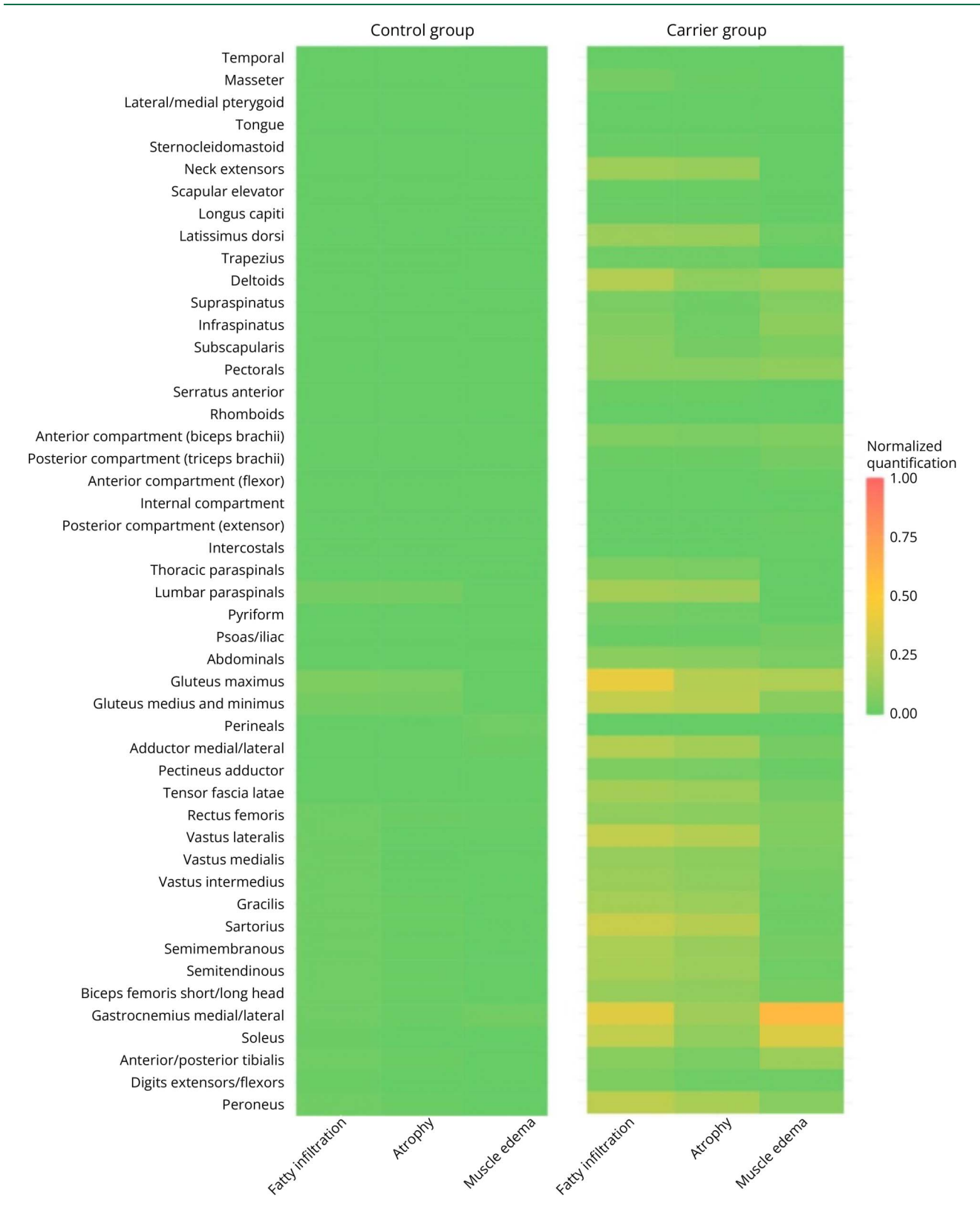
Table 1 Comparison of Demographic and Clinical Features of the DMD Carrier and Healthy Control Groups

Carriers (n = 29)	Healthy controls (n = 25)	<i>p</i> Value ^a
36 (21–65)	38 (23–56)	0.5
15 (51.7)	14 (53.8)	0.9
1.6 ± 0.1	1.6 ± 0.1	>0.9
73.6 ± 16.1	59.9 ± 8.1	<0.001
28.3 (19–45)	23.1 (17–30)	<0.001
5 (17.2)	2 (7.7)	0.4
7 (24.1)	5 (19.2)	0.7
12 (41.4)	5 (19.2)	0.076
	36 (21-65) 15 (51.7) 1.6 ± 0.1 73.6 ± 16.1 28.3 (19-45) 5 (17.2) 7 (24.1)	$36 (21-65)$ $38 (23-56)$ $15 (51.7)$ $14 (53.8)$ 1.6 ± 0.1 1.6 ± 0.1 73.6 ± 16.1 59.9 ± 8.1 $28.3 (19-45)$ $23.1 (17-30)$ $5 (17.2)$ $2 (7.7)$ $7 (24.1)$ $5 (19.2)$

Only 25 out of 30 controls completed the online form. Periodic physical activity refers to any aerobic activity performed for more than 30 min, 3 times a week during the past 3 mo.

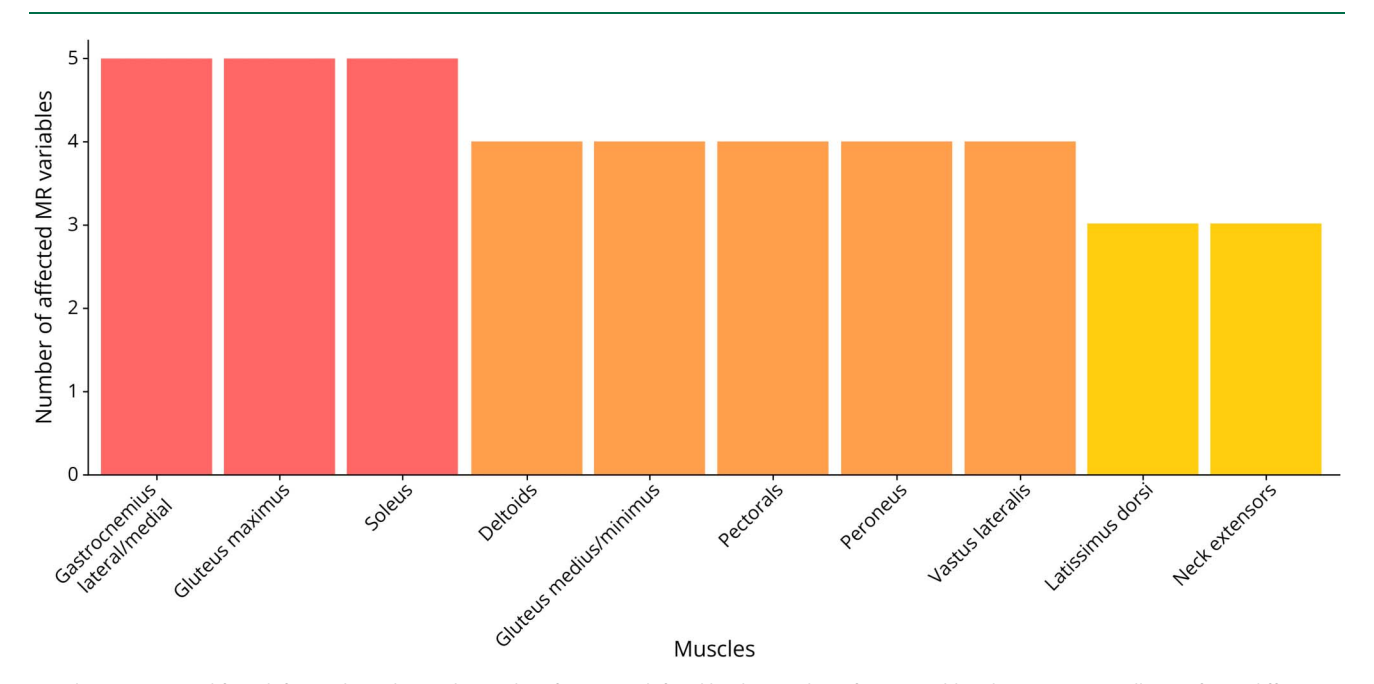
^a Wilcoxon rank-sum test; Fisher exact test; Pearson χ^2 test.

Figure 3 Heatmap Depicting the Median Normalized Quantification Values Obtained for Ordinal MRI Variables (Muscle Edema on STIR, Fatty Infiltration, and Atrophy on T1-WI) for 48 Muscles or Muscle Groups



On the left-hand side, the results from the control group, while on the right, the results from the *DMD* carrier cohort. The color gradient from green to red represents lower to higher muscle involvement, respectively. DMD = Duchenne muscular dystrophy; STIR = short-tau inversion recovery.

Figure 4 Bar Chart Illustrating the Muscles Most Affected in the DMD Carrier Group, Based on the Number of Significantly Altered MRI Variables: Edema (STIR), Fatty Infiltration, Atrophy, Pseudohypertrophy, and Texture Pattern (T1-Weighted Imaging)



Muscles are arranged from left to right in descending order of severity, defined by the number of MRI variables showing statistically significant differences between carriers and controls. DMD = Duchenne muscular dystrophy; STIR = short-tau inversion recovery.

Muscles that had an edema score greater than 0 in female carriers and showed significant differences compared with the control group's score were predominantly located in the calves, pelvic girdle, shoulder girdle, and arms (p < 0.05). The most frequently affected muscles were gastrocnemius (100%), soleus (55%), gluteus maximus (41%), deltoids (38%), tibialis anterior and posterior (31%), infraspinatus (24%), gluteus medius/minimus (20%), pectorals (17%), peroneus (17%), biceps brachii (17%), and vastus lateralis (17%) (eTable 7). None of the evaluated muscles exhibited grade III edema.

Muscles with a fatty infiltration score greater than 0 that showed statistically significant differences between groups were located in the neck, shoulder girdle, anterior compartment of the arms, abdominal wall, pelvic girdle, thighs, and calves (p < 0.05). Those muscles were gluteus maximus (100%), gastrocnemius (96.5%), soleus (76%), vastus lateralis (72.5%), gluteus medius and minimus (69%), sartorius (69%), peroneus (65%), adductor magnus/large (55%), deltoids (52%), semimembranosus (52%), semitendinosus (48%), gracilis (45%), biceps femoris (41%), tensor fascia latae (38%), neck extensors (38%), latissimus dorsi (38%), vastus medialis (34.5%), vastus intermedius (34.5%), abdominals (24%), biceps brachii (21%), pectorals (20.5%), and subscapularis (17%) (eTable 8).

The predominant textures of muscles with significant fatty infiltration in female carriers were "mottled" and "in bands" (p < 0.05). The pattern "in bands" was most prevalent in the

gluteus maximus (76%), gluteus medius and minimus (48.5%), soleus (45%), and subscapularis (10%). The "mottled" pattern was most common in gastrocnemius (55%), sartorius (55%), vastus lateralis (38%), adductor magnus/large (38%), gracilis (38%) deltoids (35%), semimembranosus (35%), biceps femoris (31%), neck extensors (28%), semitendinosus (27.5%), latissimus dorsi (27.5%), tensor fascia latae (24%), vastus intermedius (20.5%), vastus medialis (17.5%), abdominals (13.5%), and pectorals (13.5%). The biceps brachii showed an equal distribution of "in bands" and "mottled" patterns, with 7% each. The "perifascial" pattern was present only in peroneus (36%), vastus lateralis (20.5%), biceps brachii (4%), and vastus medialis (3.5%). None of the evaluated muscles showed a "porcelain" pattern of fatty infiltration (eTable 9).

Muscles with an atrophy score greater than 0 in female carriers that showed significant differences compared with the control group's score were predominantly located in the calves, pelvic girdle, shoulder girdle, and arms (p < 0.05). Those muscles were gluteus medius/minimus (65.5%), vastus lateralis (65.5%), sartorius (62%), gluteus maximus (58.5%), peroneus (55%), adductor magnus/large (48%), gastrocnemius (41%), semimembranosus (41%), semitendinosus (41%), gracilis (41%), latissimus dorsi (38%), neck extensors (38%), biceps femoris (34.5%), tensor fascia latae (31%), soleus (31%), deltoids (31%), vastus intermedius (31%), vastus medialis (31%), rectus femoris (27.5%), abdominals (24%), and pectorals (20.5%) (eTable 10).

Table 2 Analysis of the Proportion of Individuals per Group Exhibiting Involvement of the Topmost Affected Muscles, According to 4 MRI Variables

Muscle	Carriers (n = 29) (%)	Controls (n = 30) (%)	<i>p</i> Value ^s
Gastrocnemius			
Edema	29 (100)	2 (7)	<0.001
Fatty infiltration	28 (97)	2 (7)	<0.001
Atrophy	12 (41)	1 (3)	0.001
Pseudohypertrophy	17 (59)	0 (0)	<0.001
Gluteus maximus			
Edema	12 (41)	0 (0)	<0.001
Fatty infiltration	29 (100)	5 (17)	<0.001
Atrophy	17 (59)	4 (13)	0.001
Pseudohypertrophy	10 (34.5)	0 (0)	<0.001
Soleus			
Edema	16 (55)	0 (0)	<0.001
Fatty infiltration	22 (76)	1 (3)	<0.001
Atrophy	9 (31)	0 (0)	0.001
Pseudohypertrophy	17 (59)	0 (0)	<0.001
Deltoids			
Edema	9 (31)	0 (0)	<0.001
Fatty infiltration	15 (52)	0 (0)	<0.001
Atrophy	9 (31)	0 (0)	0.001
Pseudohypertrophy	0 (0)	0 (0)	0.896
Gluteus med and min			
Edema	6 (20)	0 (0)	0.01
Fatty infiltration	20 (69)	10 (3)	<0.001
Atrophy	19 (65)	10 (3)	<0.001
Pseudohypertrophy	0 (0)	0 (0)	0.896
Pectorals			
Edema	5 (17)	0 (0)	0.024
Fatty infiltration	6 (20)	0 (0)	0.011
Atrophy	6 (20)	0 (0)	0.011
Pseudohypertrophy	0 (0)	0 (0)	0.896
Peroneus			
Edema	5 (17)	0 (0)	0.024
Fatty infiltration	19 (65)	2 (7)	<0.001
Atrophy	16 (55)	1 (3)	<0.001
Pseudohypertrophy	0 (0)	0 (0)	0.896
Vastus lateralis			
Edema	5 (17)	0 (0)	0.024
			Continued

Table 2 Analysis of the Proportion of Individuals per Group Exhibiting Involvement of the Topmost Affected Muscles, According to 4 MRI Variables (continued)

Muscle	Carriers (n = 29) (%)	Controls (n = 30) (%)	<i>p</i> Value ^a
Fatty infiltration	21 (72)	2 (7)	<0.001
Atrophy	19 (66)	0 (0)	<0.001
Pseudohypertrophy	0 (0)	0 (0)	0.896
Latissimus dorsi			
Edema	1 (3.5)	0 (0)	0.492
Fatty infiltration	11 (38)	0 (0)	<0.001
Atrophy	11 (38)	0 (0)	0.001
Pseudohypertrophy	0 (0)	0 (0)	0.896
Neck extensors			
Edema	0 (0)	0 (0)	0.896
Fatty infiltration	11 (38)	0 (0)	<0.001
Atrophy	11 (38)	0 (0)	0.001
Pseudohypertrophy	0 (0)	0 (0)	0.896

Data are presented as the number of individuals, with percentages in parentheses. The MRI variables analyzed include edema, fatty infiltration, atrophy, and pseudohypertrophy in various muscles. The texture pattern variable was not included because it consistently showed significant alterations (p < 0.05) in all cases where fatty infiltration differed between groups.

^a χ^2 test; Fisher exact test.

The only muscles exhibiting pseudohypertrophy in female carriers were the medial/lateral gastrocnemius (59%), soleus (59%), and gluteus maximus (34%) (p < 0.05). No muscles exhibited true hypertrophy.

Overall, muscle severity in *DMD* female carriers frequently involved gastrocnemius, gluteus maximus, and soleus (Figure 4). The most representative WB-MRI findings in carriers are shown in Figure 6.

MRI vs Neurologic Examination

We evaluated the correlation between manual muscle strength testing and atrophy score on T1-WI. The deltoid was the only muscle depicting a statistically significant negative correlation (p = 0.042), suggesting that higher atrophy levels are associated with lower muscle strength (eFigure 1A). However, the summation of atrophy values on T1-WI and manual strength testing showed no significant correlation (eFigure 1B).

MRI vs CK

Serum CK levels were above the upper normal limit in 58.6% (17/29) of *DMD* carriers, ranging from 173 IU/L to 2,362 IU/L. Only 3 of these women also presented increased serum CK-MB values, suggesting that, in most cases, CK release might be due to skeletal muscle injury. No statistically significant correlations were observed between serum CK and muscle edema on STIR, atrophy or fatty infiltration on T1-WI (eFigure 2), or age (data not shown).

MRI vs DMD Variants

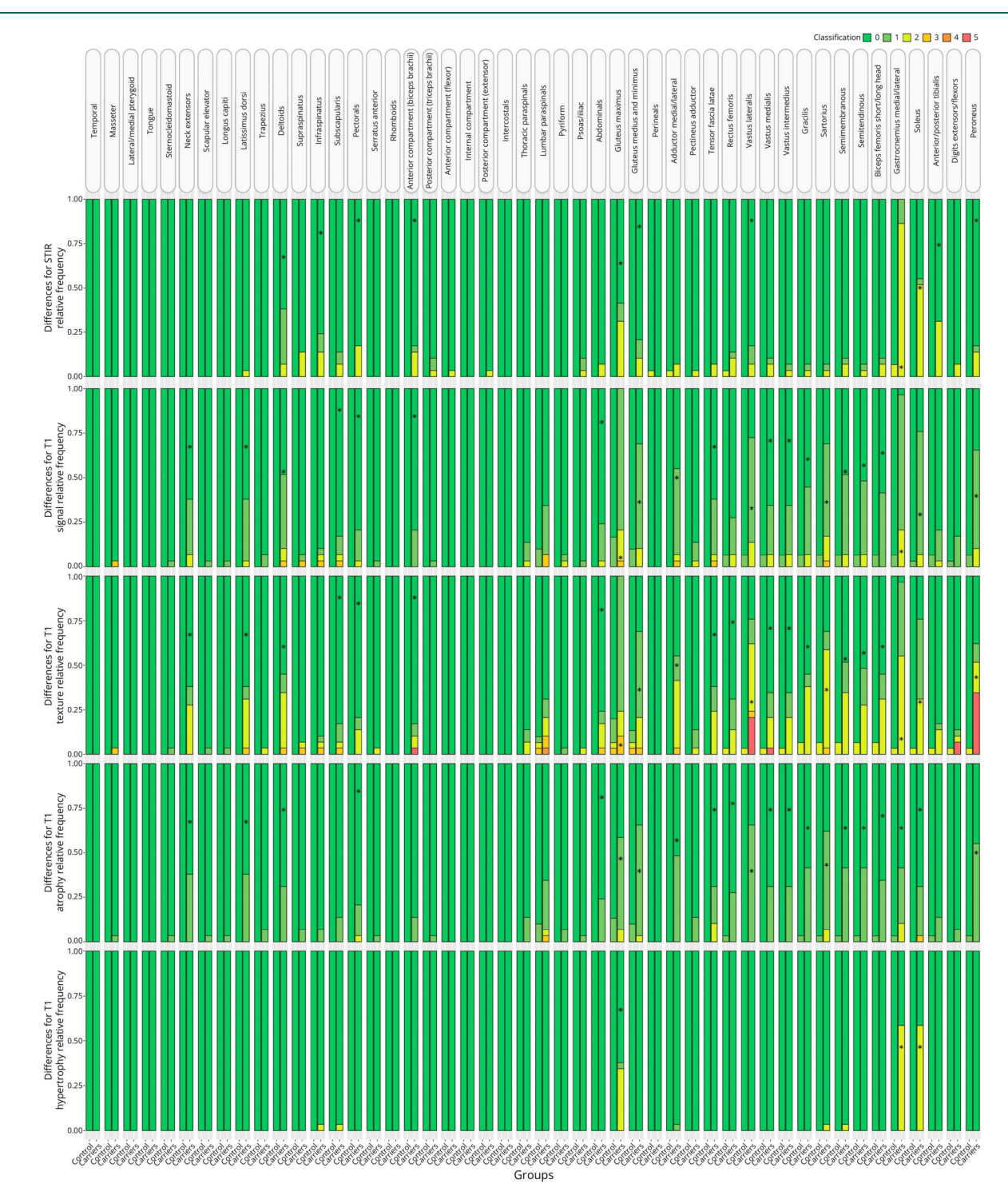
All women in the carrier group carried heterozygous *DMD* disease-causing variants (eTable 6). Based on the variants' predicted effect on dystrophin's expression and functionality, the carriers' expected phenotypes were classified as mild (6), moderate (3), and severe (20). No correlation was found between the predicted phenotype and the degree of fatty infiltration and atrophy on T1-WI, or the degree of muscle edema on STIR. The correlation between the predicted severity of *DMD* variants and STIR summation is shown in eFigure 3.

Last, we examined the correlation between blood-derived XIPs and abnormal MRI results. Most *DMD* carriers (91.7%, 22/24) presented random inactivation patterns while both remaining women exhibited moderately and highly skewed XIPs, respectively. Therefore, the presence of muscle involvement on the MRI does not appear to be associated with XIPs preferentially inactivating the reference allele.

Discussion

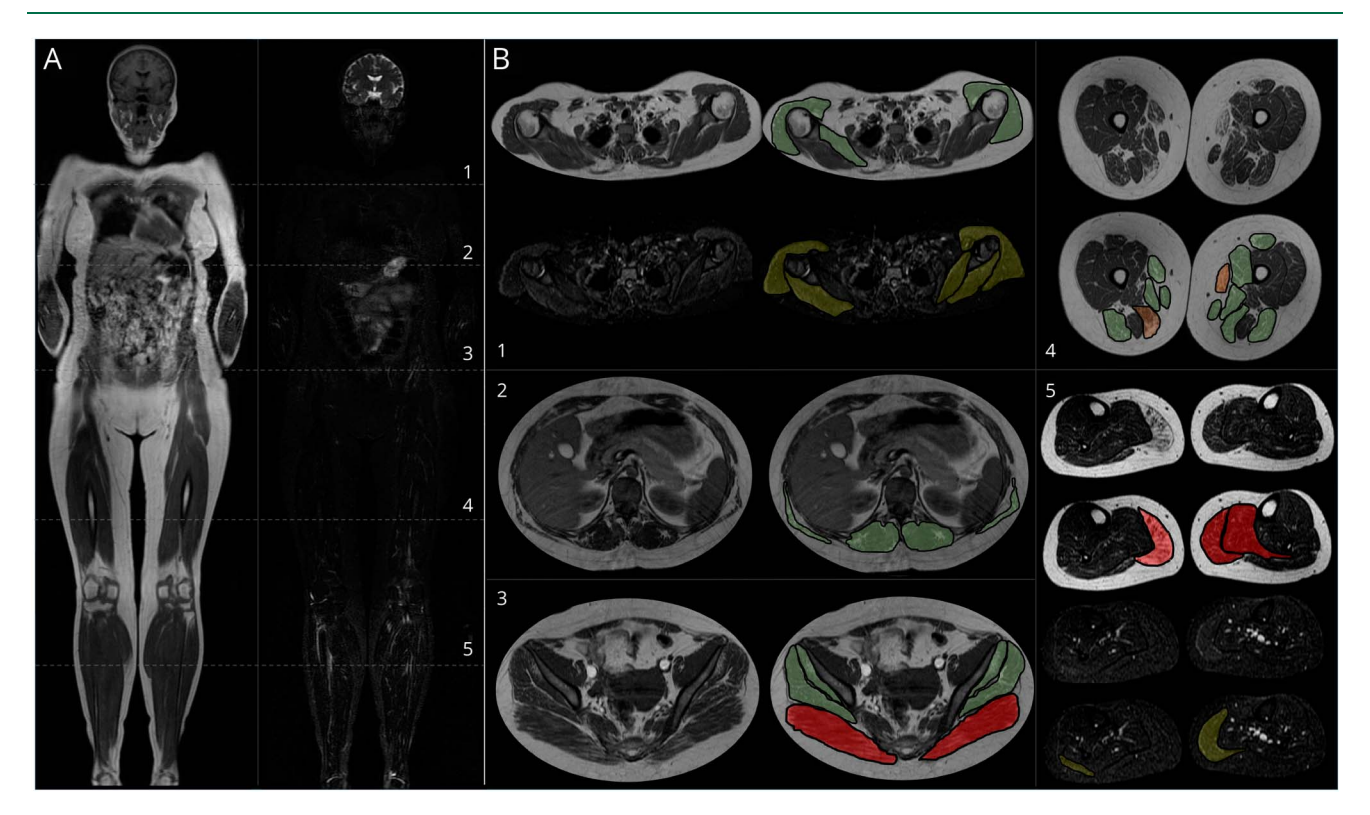
Currently, standards of care for *DMD* carriers focus solely on regular cardiologic examinations. However, current lines of investigation in various X-linked recessive diseases demonstrate the presence of variable levels of symptoms among women carrying a single pathogenic variant. ⁹⁻¹⁴ Therefore,

Figure 5 Differences in Muscle Involvement Levels Between DMD Carriers (cr) and Controls (ct)



The stacked bar chart shows the comparison of muscle involvement results obtained for each MRI variable across 48 muscles or muscle groups. The 5 evaluated MRI variables include muscle edema on STIR and fatty infiltration, texture, atrophy, and hypertrophy/pseudohypertrophy on T1-WI. Based on institutional qualitative grading scales, a color gradient from green to orange indicates increasing severity of muscle involvement across all variables, except for T1 texture, where red color denotes perifascial fatty infiltration. Muscle edema on STIR is classified as 0: normal, 1: perifascial hypersignal (hypersignal between the muscle and its fascia), 2: mild (intramuscular hypersignal in <50% of the muscle), and 3: severe (intramuscular hypersignal in >50% of the muscle). Fatty infiltration is classified as 0: normal, 1: mild (areas of high signal in <30% of the muscle), 2: moderate (areas of high signal in 30%-60% of the muscle), and 3: severe (areas of high signal in >60% of the muscle). Muscle texture is classified as 0: normal, 1: bands (linear arrangement of fatty infiltration), 2: mottled (dotted arrangement of fatty infiltration), 3: water band type (severe fatty infiltration with residual muscle fibers), 4: porcelain type (final stage, with severe muscle fatty infiltration where only neurovascular tissue and fascial border are distinguished), and 5: perifascial involvement (fatty infiltration arranged between the muscle and its fascia). T1 atrophy is subdivided into 0: normal, 1: mild (decrease in muscle volume <30%), 2: moderate (decrease in muscle volume in 30%–60%) and 3: severe (decrease in muscle volume >60%). T1 muscle trophism is classified as 0: normal, 1: true hypertrophy, and 2: pseudohypertrophy. Asterisks indicate statistically significant differences between groups (p < 0.05). Of the 240 comparisons performed, 33% showed significant differences between female groups. DMD = Duchenne muscular dystrophy; STIR = short-tau inversion recovery.

Figure 6 Representative Findings in WB-MRI of a DMD Carrier in Her Twenties



(A) Coronal pasting on T1-Wl and STIR images. (B) Axial T1-Wl and STIR images at (1) shoulder girdle, (2) chest and abdomen, (3) pelvic girdle, (4) thighs, and (5) calves. Most muscles present mild atrophy and fatty infiltration (green), observed in both deltoids and right subscapularis muscle (B1); paraspinal muscles and both latissimus dorsi (B2); both gluteus medius and minimus (B3); and left rectus femoris, semimembranosus, right sartorius, both gracilis, biceps femoris, and adductor magnus muscles (B4). Moderate-to-severe atrophy and fatty infiltration (orange) are seen in the right semimembranosus muscle and left sartorius muscle (B4). Pseudohypertrophy with fatty infiltration (red) is seen in both gluteus maximus, medial gastrocnemius, and left soleus (B3 and B5). Perifascial and intramuscular edema (yellow) are observed in both deltoids, infraspinatus and left subscapularis (B1), right lateral gastrocnemius, and left medial gastrocnemius (B5). DMD = Duchenne muscular dystrophy; STIR = short-tau inversion recovery; WB-MRI = whole-body MRI.

our primary goal was to elucidate the level of skeletal muscle involvement that DMD carriers exhibit to raise awareness and encourage the development of new care standards. Thus, we characterized and compared muscle structure between DMD carriers and female controls using qualitative analysis of WB-MRI. Although only 55% of the studied DMD carriers were symptomatic, we demonstrated that all exhibited MRI abnormalities. Carriers showed a larger proportion of muscle involvement compared with controls (85% vs 27%, p < 0.001), with muscle edema, fatty infiltration, and atrophy in 62.5% vs 8%, 81% vs 35%, and 81% vs 25%, respectively (all p < 0.001).

Carriers exhibited an asymmetric and distinctive pattern of muscle involvement, predominantly affecting muscles in the calves, thighs, and pelvis, such as gastrocnemius, soleus, gluteus maximus/medius/minimus, vastus, adductor magnus, and biceps femoris. Most carriers showed mild atrophy (50%–60%) and mild-to-moderate fatty infiltration (65%–95%) (p < 0.001). The presence of degenerative signs in lower-extremity muscles in DMD carriers has also been described, 9 yet comparison of results is hampered because of different types of MRI analysis. Two other

publications, focusing principally on female dystrophinopathy patients, observed similar patterns of muscle involvement. Observed similar patterns of muscle involvement. Severe involvement of the medial gastrocnemius, adductor magnus, biceps femoris long head, and vastus has been described. In women with heterozygous DMD variants, the most affected muscles are the quadratus femoris, adductor magnus, biceps femoris long head, and gluteus maximus, followed by the semi-membranosus, gastrocnemius medialis, and vastus, with the gluteus maximus/medius, adductor magnus, tensor fasciae lata, and soleus being affected in the mildest cases. While these reports focused only on fatty infiltration, we also investigated muscle edema, which was frequently detected in calves (medial/lateral gastrocnemius, soleus, peroneus) and pelvic girdle (gluteus maximus/medius/minimus). 10,25

No difference was found between groups in relation to muscle symptoms. This differs from what has been previously reported in the literature, where DMD carriers were found to experience muscle weakness more frequently than controls. Moreover, we found no correlation between the MRI results and manual muscle testing, which could be due to the subjective nature of the MRC score and its low sensitivity. This

was validated in a previous study,⁹ which found that the MRC scale was ineffective in distinguishing individuals at the mild end of the spectrum, with this distinction being achieved by dynamometry testing instead.

According to literature, 50%–70% of *DMD* carriers have increased serum CK levels and our results are consistent with these findings. The lack of correlation observed between MRI results and CK levels could be due to the age-related decrease in CK levels, which may result from aging and/or the normalization process, in which dystrophin-negative fibers getting gradually replaced with dystrophin-positive fibers by rounds of necrosis and regeneration. ²⁸

No correlation was found between *DMD* variant and WB-MRI results. Some elements could be hindering such correlation: the uncertainty in predicting the effect of variants on muscle fibers and the remaining functionality of the aberrant dystrophin²⁹; variability in dystrophin expression levels³⁰; the epistatic effect of modifier genes³¹; and the percentage of dystrophin-negative fibers in each muscle (proportion of cells expressing the reference vs the altered allele).

Most carriers presented random XIPs, indicating mosaic expression of both *DMD* alleles in muscle. The 8.7% of women with skewed patterns aligns with similar proportions seen in the general population.³² Overall, XIPs do not seem to influence the varying levels of muscle involvement among *DMD* carriers; however, these findings must be validated in muscle tissue.³³

The major asset of this study is the use of WB-MRI, which provides a thorough and clear picture of the pattern of muscle involvement in DMD carriers, whereas other studies solely analyzed the lower limbs. 9,10,25 Yet, we recognize a probable recruitment bias because the included DMD carriers were those with resources and availability to attend Fleni, excluding women with limited resources or mobility impairment. In addition, we acknowledge some limitations in our study. First, only a qualitative muscle assessment of the MRI was performed. Although a quantitative analysis could have provided more accurate and reproducible results, it is also more time-consuming because of the need for manual muscle segmentation and requires specific software that may not be available at all hospitals. Second, women in the control group did not undergo DMD genetic testing. However, given the lack of family history, the occurrence of de novo sequence variants in DMD, and the sample size, it is reasonable to assume that they do not carry DMD diseasecausing variants. Third, the DMD carrier and control groups were not BMI matched. Although the higher BMI values in the carrier group may have influenced the level of muscle involvement observed on MRI, they do not explain the specific pattern of involvement, which mirrors that seen in patients with DMD. In addition, we did not evaluate the relationship between muscle MRI findings and age in both

groups. Finally, the effect of epigenetic and environmental factors (e.g., age and the burden of caring for patients with *DMD*) was not evaluated.³⁴ Albeit true, given that 55% of the tested carriers were sisters, aunts, or grandmothers of the male proband, the impact of caregiving in this cohort is likely negligible.

In conclusion, all *DMD* carriers in our study show signs of skeletal muscle involvement on MRI. Therefore, our findings, together with recent literature, underscore the importance of raising awareness among the non-neurologic medical professionals caring for these women. ^{3,5-9} Yet, because abnormal MRI findings are known to precede symptoms in many cases, future longitudinal studies are needed to determine how frequently asymptomatic *DMD* carriers with such findings develop overt muscle weakness later in their lives, along with studies correlating skeletal muscle and cardiac manifestations, with the long-term goal of improving the care of *DMD* female carriers.

Acknowledgment

The authors are thankful to Juan Pablo Picasso, PhD, for additional statistical assessment, and the patients, their families, and the Asociación Distrofia Muscular para las Enfermedades Neuromusculares de Argentina (ADM) for the provided support.

Author Contributions

A.P. Vigliano: drafting/revision of the manuscript for content, including medical writing for content; major role in the acquisition of data; analysis or interpretation of data. L. Luce: drafting/revision of the manuscript for content, including medical writing for content; major role in the acquisition of data; analysis or interpretation of data. J.M. Pastor Rueda: drafting/revision of the manuscript for content, including medical writing for content; major role in the acquisition of data; analysis or interpretation of data. H. Chaves: drafting/ revision of the manuscript for content, including medical writing for content; analysis or interpretation of data. L. Mesa: drafting/revision of the manuscript for content, including medical writing for content. M. Carcione: drafting/revision of the manuscript for content, including medical writing for content; major role in the acquisition of data. C. Mazzanti: drafting/revision of the manuscript for content, including medical writing for content; major role in the acquisition of data. C.L. Massini: drafting/revision of the manuscript for content, including medical writing for content; major role in the acquisition of data. C.P. Radic: drafting/revision of the manuscript for content, including medical writing for content; major role in the acquisition of data. C. Cejas: drafting/ revision of the manuscript for content, including medical writing for content; major role in the acquisition of data; study concept or design; analysis or interpretation of data. F. Giliberto: drafting/revision of the manuscript for content, including medical writing for content; major role in the acquisition of data; study concept or design; analysis or interpretation of data.

Study Funding

This study was funded by the University of Buenos Aires (UBACYT: UBACyT 2020-No20020190100332BA) and PTC Therapeutics.

Disclosure

F. Giliberto and L. Mesa have received honoraria/grants for either teaching, consultation, advisory board and speaker activities from PTC Therapeutics, Sarepta Therapeutics, Sanofi Genzyme, and Biomarin. F. Giliberto received research grants from PTC pharmaceuticals to perform genetic testing of patients. H. Chaves has received honoraria/grants for either consultation, speaker activities, and traveling to conferences from Entelai LLC and Boehringer Ingelheim. C. Cejas is president of the Argentinian Society of Radiology. The sponsor did not interfere with study design; collection, analysis, and interpretation of data; writing of the manuscript; or the decision to submit the present work for publication. The remaining authors have nothing to report. Go to Neurology.org/NG for full disclosures.

Publication History

Received by *Neurology*[®] *Genetics* January 28, 2025. Accepted in final form July 22, 2025. Submitted and externally peer-reviewed. The handling editor was Editor Peter B. Kang, MD, FAAN.

References

- Hoffman EP, Brown RHJr, Kunkel LM. Dystrophin: the protein product of the Duchenne muscular dystrophy locus. Cell. 1987;51(6):919-928. doi:10.1016/0092-8674(87)90579-4
- Brandsema JF, Darras BT. Dystrophinopathies. Semin Neurol. 2015;35(4):369-384. doi:10.1055/s-0035-1558982
- Norman A, Harper P. A survey of manifesting carriers of Duchenne and Becker muscular dystrophy in Wales. Clin Genet. 1989;36(1):31-37. doi:10.1111/j.1399-0004.1989.tb03363.x
- Soltanzadeh P, Friez MJ, Dunn D, et al. Clinical and genetic characterization of manifesting carriers of DMD mutations. *Neuromuscul Disord*. 2010;20(8):499-504. doi:10.1016/j.nmd.2010.05.010
- Grain L, Cortina-Borja M, Forfar C, Hilton-Jones D, Hopkin J, Burch M. Cardiac abnormalities and skeletal muscle weakness in carriers of Duchenne and Becker muscular dystrophies and controls. *Neuromuscul Disord*. 2001;11(2):186-191. doi: 10.1016/s0960-8966(00)00185-1
- Viggiano E, Picillo E, Ergoli M, Cirillo A, Del Gaudio S, Politano L. Skewed X-chromosome inactivation plays a crucial role in the onset of symptoms in carriers of Becker muscular dystrophy. J Gene Med. 2017;19(4):e2952. doi:10.1002/jgm.2952
- Fujii K, Minami N, Hayashi Y, et al. Homozygous female Becker muscular dystrophy. Am J Med Genet A. 2009;149A(5):1052-1055. doi:10.1002/ajmg.a.32808
- Zatz M, Vianna-Morgante AM, Campos P, Diament AJ. Translocation (X;6) in a female with Duchenne muscular dystrophy: implications for the localisation of the DMD locus. J Med Genet. 1981;18(6):442-447. doi:10.1136/jmg.18.6.442
- Fornander F, Solheim TÅ, Eisum A-SV, et al. Quantitative muscle MRI and clinical findings in women with pathogenic dystrophin gene variants. Front Neurol. 2021;12: 707837. doi:10.3389/fneur.2021.707837
- Tasca G, Monforte M, Iannaccone E, et al. Muscle MRI in female carriers of dystrophinopathy. Eur J Neurol. 2012;19(9):1256-1260. doi:10.1111/j.1468-1331.2012.03753.x
- Bryant P, Boukouvala A, McDaniel J, Nance D. Hemophilia A in females: considerations for clinical management. Acta Haematol. 2020;143(3):289-294. doi:10.1159/000502890
- Pérez L. Hemophilia carriers and women with coagulopathies: challenges in the occupational arena. Blood Coagul Fibrinolysis. 2020;31(1S):S15-S16. doi:10.1097/ MBC.000000000000985

- Torii R, Hashizume A, Yamada S, et al. Clinical features of female carriers and prodromal male patients with spinal and bulbar muscular atrophy. *Neurology*. 2023; 100(1):e84-e93. doi:10.1212/WNL.000000000201342
- Cavenagh A, Chatterjee S, Davies W. Behavioural and psychiatric phenotypes in female carriers of genetic mutations associated with X-linked ichthyosis. PLoS One. 2019;14(2):e0212330. doi:10.1371/journal.pone.0212330
- Murray MG, Thompson WF. Rapid isolation of high molecular weight plant DNA. Nucleic Acids Res. 1980;8(19):4321-4325. doi:10.1093/nar/8.19.4321
- Fratter C, Dalgleish R, Allen SK, et al. EMQN best practice guidelines for genetic testing in dystrophinopathies. Eur J Hum Genet. 2020;28(9):1141-1159. doi:10.1038/ s41431-020-0643-7
- Luce L, Carcione M, Mazzanti C, et al. Theragnosis for Duchenne muscular dystrophy. Front Pharmacol. 2021;12:648390. doi:10.3389/fphar.2021.648390
- Aartsma-Rus A, Van Deutekom JCT, Fokkema IF, Van Ommen G-JB, Den Dunnen JT. Entries in the Leiden Duchenne muscular dystrophy mutation database: an overview of mutation types and paradoxical cases that confirm the reading-frame rule. Muscle Nerve. 2006;34(2):135-144. doi:10.1002/mus.20586
- Vignos PJ Jr, Spencer GE Jr, Archibald KC. Management of progressive muscular dystrophy in childhood. JAMA. 1963;184:89-96. doi:10.1001/ jama.1963.03700150043007
- Medical Research Council (Great Britain). Aids to the Examination of the Peripheral Nervous System. 1976.
- Mercuri E, Pichiecchio A, Allsop J, Messina S, Pane M, Muntoni F. Muscle MRI in inherited neuromuscular disorders: past, present, and future. J Magn Reson Imaging. 2007;25(2):433-440. doi:10.1002/jmri.20804
- Borsato C, Padoan R, Stramare R, Fanin M, Corrado A. Limb-girdle muscular dystrophies type 2A and 2B:Clinical and radiological aspects. Basic Appl Myol Epub. 2006: 17-25.
- Allen RC, Zoghbi HY, Moseley AB, Rosenblatt HM, Belmont JW. Methylation of HpaII and HhaI sites near the polymorphic CAG repeat in the human androgenreceptor gene correlates with X chromosome inactivation. Am J Hum Genet. 1992; 51(6):1229-1239.
- Amos-Landgraf JM, Cottle A, Plenge RM, et al. X chromosome-inactivation patterns of 1,005 phenotypically unaffected females. Am J Hum Genet. 2006;79(3):493-499. doi:10.1086/507565
- Forbes SC, Lott DJ, Finkel RS, et al. MRI/MRS evaluation of a female carrier of Duchenne muscular dystrophy. Neuromuscul Disord. 2012;22(suppl 2):S111-S121. doi:10.1016/j.nmd.2012.05.013
- Falcão-Conceição DN, Gonçalves-Pimentel MM, Baptista ML, Ubatuba S. Detection
 of carriers of X-linked gene for Duchenne muscular dystrophy by levels of creatine
 kinase and pyruvate kinase. J Neurol Sci. 1983;62(1-3):171-180. doi:10.1016/0022510x(83)90197-1
- Percy ME, Chang LS, Murphy EG, Oss I, Verellen-Dumoulin C, Thompson MW.
 Serum creatine kinase and pyruvate kinase in Duchenne muscular dystrophy carrier detection. *Muscle Nerve*. 1979;2(5):329-339. doi:10.1002/mus.880020503
- Sumita DR, Vainzof M, Campiotto S, et al. Absence of correlation between skewed X inactivation in blood and serum creatine-kinase levels in Duchenne/Becker female carriers. Am J Med Genet. 1998;80(4):356-361. doi:10.1002/(sici)1096-8628(19981204)80:4<356::aid-ajmg10>3.0.co;2-o
- Torella A, Zanobio M, Zeuli R, et al. The position of nonsense mutations can predict the phenotype severity: a survey on the DMD gene. PLoS One. 2020;15(8):e0237803. doi:10.1371/journal.pone.0237803
- Beekman C, Janson AA, Baghat A, van Deutekom JC, Datson NA. Use of capillary Western immunoassay (Wes) for quantification of dystrophin levels in skeletal muscle of healthy controls and individuals with Becker and Duchenne muscular dystrophy. PLoS One. 2018;13(4):e0195850. doi:10.1371/journal.pone.0195850
- Bello L, Pegoraro E. The "usual suspects": genes for inflammation, fibrosis, regeneration, and muscle strength modify Duchenne muscular dystrophy. J Clin Med. 2019;8(5):649. doi:10.3390/jcm8050649
- Shvetsova E, Sofronova A, Monajemi R, et al. Skewed X-inactivation is common in the general female population. Eur J Hum Genet. 2019;27(3):455-465. doi:10.1038/ s41431-018-0291-3
- Brioschi S, Gualandi F, Scotton C, et al. Genetic characterization in symptomatic female DMD carriers: lack of relationship between X-inactivation, transcriptional DMD allele balancing and phenotype. BMC Med Genet. 2012;13:73. doi:10.1186/ 1471.3360.13.73.
- Pangalila RF, van den Bos GAM, Stam HJ, van Exel NJA, Brouwer WBF, Roebroeck ME. Subjective caregiver burden of parents of adults with Duchenne muscular dystrophy. Disabil Rehabil. 2012;34(12):988-996. doi:10.3109/09638288.2011.628738